The American Journal of Pathology, Vol. 175, No. 6, December 2009

DOI: 10.2353/ajpath.2009.090130

Neurobiology

Brain-Specific Deletion of Extracellular Signal-Regulated Kinase 2 Mitogen-Activated Protein Kinase Leads to Aberrant Cortical Collagen Deposition

Daniel S. Heffron,* Gary E. Landreth,†
Ivy S. Samuels,† and James W. Mandell*

From the Department of Pathology, University of Virginia School of Medicine, Charlottesville, Virginia; and the Alzheimer's Research Laboratory,† Case Western Reserve University School of Medicine, Cleveland, Ohio*

The mitogen-activated protein kinases extracellular signal-regulated kinase (ERK)1 and 2 are essential intracellular mediators of numerous transmembrane signals. To investigate neural-specific functions of ERK2 in the brain, we used a Cre/lox strategy using *Nestin:Cre* to drive recombination in neural precursor cells. *Nestin:Cre*;ERK2$^{fl/fl}$ conditional knockout (cKO) mice have architecturally normal brains and no gross behavioral deficits. However, all cKO mice developed early-onset (postnatal day 35 to 40) frontal cortical astrogliosis, without evidence of neuronal degeneration. Frontoparietal cortical gray matter, but not underlying white matter, was found to contain abundant pericapillary and parenchymal reticulin fibrils, which were shown by immunohistochemistry to contain fibrillar collagens, including type I collagen. ERK1 general KO mice showed neither fibrils nor astrogliosis, indicating a specific role for ERK2 in the regulation of brain collagen. Collagen fibrils were also observed to a lesser extent in *GFAP:Cre*;ERK2$^{fl/fl}$ mice but not in *CamKII-Cre*;ERK2$^{fl/fl}$ mice (pyramidal neuron specific), consistent with a possible astroglial origin. Primary astroglial cultures from cKO mice expressed elevated fibrillar collagen levels, providing further evidence that the phenotype may be cell autonomous for astroglia. Unlike most other tissues, brain and spinal cord parenchyma do not normally contain fibrillar collagens, except in disease states. Determining mechanisms of ERK2-mediated collagen regulation may enable targeted suppression of glial scar formation in diverse neurological disorders. *(Am J Pathol 2009, 175:2586–2599; DOI: 10.2353/ajpath.2009.090130)*

The extracellular signal-regulated kinase (ERK) family of mitogen-activated protein kinases (MAPKs) has been intensely studied for roles in brain development, including control of both axonal[1,2] and dendritic[3] growth. Astroglial process extension is also dependent on ERK signaling.[4] Recent work strongly implicates ERK-mediated signaling in synaptic plasticity and memory formation, and mutations in ERK2 and other ERK pathway components are known to underlie some forms of inherited human cognitive disorders.[5–7] ERK MAPK activation is also linked to astroglial activation in several forms of central nervous system (CNS) injury.[8–10]

To directly test the importance of ERK MAPKs *in vivo*, gene knockout approaches are needed. Whereas ERK1 general knockout (KO) mice are viable and have architecturally normal brains,[11] general KO of ERK2 is embryonic lethal, because of defects in mesoderm differentiation and placental development.[12–14] Thus, conditional KO (cKO) strategies are necessary to study brain-specific roles of ERK2. Two recent reports[15,16] describe aspects of the developmental phenotype resulting from CNS-specific KO of the *mapk1* gene, encoding ERK2. We now present a novel aspect of the adult phenotype of a brain-specific ERK2 cKO driven by *Nestin:Cre*. Our findings suggest an unexpected and specific role for this classical MAPK member in the regulation of brain collagen deposition.

Materials and Methods

Transgenic Mice and PCR Genotyping

The generation of strain harboring a conditional ("floxed") *mapk1* mutant allele (*Mapk1$^{flox/flox}$*; subsequently referred

Supported by grants NS047378 (to J.W.M.) and NS032779, MH57014, NS13546, and NS057098 (to G.E.L.).

Accepted for publication August 20, 2009.

Supplemental material for this article can be found on *http://ajp.amjpathol.org*.

Address reprint requests to James W. Mandell, M.D., Ph.D., Department of Pathology, P.O. Box 800904, University of Virginia, Charlottesville, VA 22908. E-mail: jwm2m@virginia.edu.

to as ERK2$^{fl/fl}$) was reported previously.[15] Floxed ERK2 mice were maintained as heterozygotes. *Nestin:Cre* mice were maintained on a C57BL/6 background (Jax catalog number 003771; The Jackson Laboratory, Bar Harbor, ME). Breeding pairs consisted of male *Nestin:Cre/+;* ERK2 $^{fl/+}$ mated with female *+/+;*ERK2 $^{fl/fl}$. Genotyping for the presence of Cre recombinase consisted of the following reaction: forward primer, 5′-GGTCGATGCAACGAGTGATGAGG-3′, and reverse primer, 5′-GCTAAGTGCCTTCTCTACACCTGCG-3′; reaction conditions: 2 mmol/L $MgCl_2$, 400 nmol/L primers, 200 nmol/L 2′-deoxynucleoside 5′-triphosphates, and 0.025 U/μl Taq (Qiagen 201203; Qiagen, Valencia, CA); and thermocycle conditions: 94°C for 3 minutes, 94°C for 30 seconds, 51°C for 1 minute, 72°C for 1 minute, and 72°C for 2 minutes, with 35 amplification cycles. This results in a 550-bp product, which is only present after cre-mediated excision of the floxed allele. TrkB cKO mouse brain tissue was a gift from Dr. L. Reichardt (University of California, San Francisco, San Francisco, CA).

Mouse Brain Magnetic Resonance Imaging

Magnetic resonance imaging (MRI) was performed on adult male mice (4 to 6 months) using a 4.7-T MRI scanner (Varian, Palo Alto, CA). T1-weighted coronal scans were obtained both pre- and postgadolinium injection, and the latter used to detect possible vascular abnormalities and/or blood-brain-barrier dysfunction.

Behavioral Tests

Adult male mice (4 to 6 months) were used for all behavioral tests. Animals were housed with *ad libitum* access to food and water, maintained on a 12-hour light/dark cycle and under controlled temperature and humidity. All experiments were performed in accordance with the University of Virginia Animal Care and Use Committee. Open-field locomotion and exploratory behavior in a novel environment was conducted on three wild-type and three ERK2 cKO littermate mice. The test consisted of placing each mouse in the corner of a 60 × 60 cm activity cage (VersaMax Animal Activity Monitoring System; AccuScan Instruments, Columbus, OH) for a 15-minute test session. Activity was defined as total horizontal distance traveled in centimeters. Exploratory behavior was defined as the number vertical beam breaks times the beam's elevation (5 cm) from the floor. Data were acquired and processed using Versamax software. For the tail suspension test, three wild-type and three cKO littermate mice were suspended by the tail for 6 minutes and video recorded using a webcam (Logictech, Fremont, CA). Behavioral despair was scored as the total time of immobility. Mice were considered immobile when hanging motionless with their limbs tucked into their body.

Significance of differences between genotypes was assessed using Student's *t*-test.

Cell Culture

Neonatal primary astrocyte cultures were prepared as described previously.[9] Briefly, the forebrain was dissected from newborn pups, meninges were removed, and cells were dissociated in 0.05% trypsin EDTA for 5 minutes at 37°C. Following trituration, cells were pelleted and resuspended in Dulbecco's modified Eagle's medium supplemented with 10% fetal bovine serum, penicillin (50 U/ml), and streptomycin (50 μg/ml) (all from Invitrogen, Carlsbad, CA). Media were replaced twice per week for 2 weeks to obtain standard astroglial monolayers.

Tissue Processing

Mice were anesthetized with a lethal dose of pentobarbital and transcardially perfused at room temperature with 10 ml of PBS, followed by 10 ml of PBS/4% paraformaldehyde over a period of 3 to 5 minutes. Brains were fixed for 24 hours at 4°C. For Gallyas silver staining, brains were allowed to postfix *in situ* before removal the next day, followed by an additional 3 to 8 days of fixation at 4°C. After equilibrating in 30% sucrose for 48 hours, 40-μm free-floating cryosections were collected using a sliding microtome. Alternatively, brains were processed for paraffin infiltration by standard methods. All animal procedures were approved by the University of Virginia Animal Care and Use Committee.

Electron Microscopy

Blocks of frontal cortices of cKO and wild-type animals, after initial perfusion fixation with 4% paraformaldehyde, were postfixed in 2% glutaraldehyde/0.1 M cacodylate buffer overnight at 4°C. Tissues were dehydrated and processed into Epon resin using standard techniques. Ultrathin sections were stained with uranyl acetate and viewed and photographed on a JEOL 1200 electron microscope.

Western Blotting

Astrocyte cultures or brain lysates were lysed directly in Laemmli sample buffer and separated by electrophoresis using standard procedures. Gels were transferred to polyvinylidene difluoride for 90 minutes with a semidry transfer apparatus and blocked with either a commercial blocking reagent (LI-COR block; LI-COR, Lincoln NE) for infrared imaging or 5% milk powder for chemiluminescent imaging. Blots were blocked overnight at 4°C, then probed with primary antibodies (glial fibrillary acidic protein (GFAP), 1/20,000 (Dako, Carpinteria, CA); α-tubulin, 1/4,000 (Sigma-Aldrich, St. Louis, MO); total ERK1/ERK2, 1/5,000 (Sigma-Aldrich); and ERK2, 1/5,000 (Upstate Biotechnology, Lake Placid, NY)) for 1 hour at room temperature. Secondary antibodies were goat anti-mouse IRDye800 and goat anti-rabbit Cy5.5 (Rockland, Gilbertsville, PA) at 1/2000 for infrared imaging, or horse anti-mouse horseradish peroxidase (A4416; Sigma-Aldrich). Blots using the former secondaries were imaged and quantified on

Table 1. Primary Antibodies Used in Immunohistochemical, Immunofluorescence, and Western Blotting Experiments

Antigen	Antibody name/clone	Host species	Dilution WB	Dilution IHC/IF	Company	Catalog no.
α-Synuclein	α-Synuclein	Sheep		1/2,000	Chemicon International, Temecula, CA	AB5334P
5-Bromo-2′-deoxyuridine	BU1/75 (ICR1)	Rat		1/100	Abcam	6326
CD11B	Mac1	Rat		1/100	BD Pharmingen, San Diego, CA	550282
Cleaved caspase 3	Asp175	Rabbit		1/100	Cell Signaling Technology, Beverly, MA	9661
ERK2	1B3B9	Mouse	1/5,000	1/500	Upstate Biotechnology	05-157
Phospho-ERM	Phospho-ERM	Rabbit		1/400	Cell Signaling Technology	3141
F4/80	CI:A3-1	Rat		1/100	Serotec, Oxford, U.K.	MCA497
MAP2	AP18	Mouse		1/200	Binder, L.	
GFAP	GFAP	Rabbit	1/25,000	1/5,000	Dako	Z0334
Nestin	nestin	Mouse		1/50	DSHB	Rat 401
Neurofilament dephospho	SMI 32R	Mouse		1/1,000	Covance Research Products, Denver, PA	SMI 32R
Proliferating cell nuclear antigen	PC10	Mouse		1/1,000	Oncogene	NA03T
pERK	MAPK-YT	Mouse		1/500	Sigma-Aldrich	M8159
Tau	PHF1	Mouse		1/500	ICN	PHF1
Phosphorylated neurofilament	SMI 31	Mouse		1/500	Covance	SMI 31
SV2	SV2	Mouse		1/10	DSHB	SV2
Tau AT 8	Tau AT 8	Mouse		1/1,000	Pierce, Rockford, IL	MN1020
Tau AT 180	Tau AT 180	Mouse		1/2,000	Pierce	MN1040
Tau1		Mouse		1/1,000	Chemicon International	3420
Total ERK		Rabbit	1/5,000	1/500	Sigma-Aldrich	M5670
Tubulin		Mouse	1/5,000	1/5,000	NeoMarkers	MS 581 P1
Ubiquitin		Rabbit		1/2,000	Dako	Z0458
Vimentin	VIM-13.2	Mouse		1/2,000	Sigma-Aldrich	V5255
CD31	MEC13.3	Mouse		1/50	BD Pharmingen	550274
Collagen IV		Rabbit		1/500	Chemicon International	AB756P
F1C3	F1C3	Mouse	1/1,000	1/200	Faisner, A.	
MLC1	MLC1	Rabbit		1/100	Estevez, R.	
Neurofilament	2H3	Mouse		Neat	DSHB	2H3

WB, Western blotting; IHC, immunohistochemistry; IF, immunofluorescence.

an Odyssey LI-COR infrared scanner. Chemiluminescent blots were imaged with Pierce Supersignal (Pierce 34080) on Classic Blue BX film from Midwest Scientific.

Immunohistochemistry and Special Stains

Free floating frozen sections or paraffin sections prepared as described above were processed for immunohistochemistry using standard techniques, as previously described.[9] Immunostaining for collagen IV required pepsin pretreatment, as described previously.[17] Detailed information on all primary antibodies including dilutions for immunohistochemistry is provided in Table 1. Immunohistochemical detection was performed using the Vector ABC Elite kit (Vector Laboratories, Burlingame, CA), according to the supplier's instructions. The chromogen used was diaminobenzidine (S3000; Dako) 1 mg/ml in PBS plus 0.02% hydrogen peroxide applied for 3 minutes. Brightfield images were acquired with an Olympus BX40 upright microscope and a Scion Firewire CCD camera (Scion, Frederick, MD). Images within each figure were acquired to Photoshop 7.0 with the same exposure parameters to allow for comparisons of intensity. Gallyas silver stain was performed as described previously.[18] This method is used to visualize degenerating synaptic terminals, processes, and cell bodies of neurons that become argyrophilic during the process of cell death by unknown chemical mechanisms. The staining procedure entails alkaline pretreatment, silver impregnation, development at pH between 5.5 and 6.3, washing in acetic acid, and dehydration. Thioflavine S staining was performed as described previously.[19] Antibodies used for immunohistochemistry and/or Western blotting are listed in Table 1.

GFAP Immunohistochemistry and Quantification

GFAP immunohistochemistry was quantified according to a previously published method.[20] Brain tissue from littermates

was processed identically and simultaneously from perfusion to imaging. Brightfield images of paraffin or floating sections were taken on an Olympus BX40 with identical exposures and camera settings. Using ImageJ 1.32 (W. Rasband, National Institute of Mental Health, Bethesda, MD; downloaded 11/1/2008 from http://rsb.info.nih.gov/ij/index.html), images were separated into their red, green, and blue components and the blue image (best representing diaminobenzidine signal) was thresholded and binarized. Two regions of interest of constant dimensions were chosen, one in frontal cortex and one in subjacent corpus callosum (control region). The latter was chosen as a control region because the levels of GFAP immunoreactivity did not vary between cKO and controls in this region.

Microarray Analysis

Total RNA was prepared using the RNeasy™ tissue kit (Qiagen) from frontal cerebral cortex of three adult male homozygous null ERK2 cKO mice, and three adult male littermates (genotypes: +/+; fl/fl, Cre/+; +/+, +/+; and fl/+). cDNA labeling, hybridization, scanning, and data analysis were performed by the Duke Microarray Facility under contract from the National Institutes of Health Neuroscience Microarray Consortium. Dye-labeled cDNA was hybridized on Affymetrix whole-genome GeneChip Mouse Gene 1.0 ST arrays. The fold ratio of ERK2 cKO versus wild type for each probe was statistically analyzed by analysis of variance and considered significant at $P < 0.05$.

Results

Generation and Characterization of a Nestin Promoter-Directed ERK2 Conditional Mutant

A floxed allele in which exon 2 of ERK2 is flanked by two loxP sites was constructed as reported previously.[16] *Nestin:Cre* transgenic mice, in which Cre is expressed under the control of the promoter and the nervous system-specific enhancer within the second intron of the nestin gene, have been extensively characterized in numerous publications since their initial development.[21] This Cre line drives recombination in the vast majority (>90%) of central nervous system neurons and macroglia (astrocytes and oligodendrocytes but not mesoderm-derived microglia or vascular cells), as previously demonstrated with three different Cre-reporter lines.[22] Female mice homozygous for the floxed allele (*ERK2* $^{fl/fl}$) were mated with males heterozygous for *Nestin:Cre*, resulting in litters composed of +/+ (wild type for ERK2), −/+ (heterozygous ERK2 KOs), and −/− (homozygous ERK2 KOs, referred to as cKO). In one set of crosses, *GFAP:Cre*[23] males were mated with female mice homozygous for the floxed ERK2 allele.

Successful recombination of the floxed ERK2 locus in neural tissues of progeny from ERK2$^{fl/fl}$ × *Nestin:Cre* crosses (homozygous null cKOs are hereafter referred to as ERK2 cKO mice) was confirmed both in primary cortical astroglial cultures and brain tissue (Figure 1). A PCR-based recombination assay demonstrated proper recombination at the DNA level in postnatal cerebellar tissue and, as a positive control, in cortical astroglial cultures (ERK2$^{fl/fl}$) infected with adenovirus expressing Cre recombinase (Figure 1A). Loss of ERK2 protein in cultures (Figure 1B) and brain tissue (Figure 1, C–G) was confirmed by Western blot analysis and immunohistochemistry. Importantly, Western blotting with a pan-ERK (ERK1 and ERK2) antibody showed no compensatory up-regulation of ERK1 in brain tissues of cKO mice at all ages examined (3 weeks, 5 weeks, and 6 months). Immunohistochemistry with an ERK2-specific antibody in control animals showed widespread expression, with highest levels in cortex, hippocampus, and striatum. Intense staining was found in neuropil and neuronal somata (Figure 1F). cKO brains showed complete loss of ERK2 immunoreactivity in most brain regions (Figure 1E), in keeping with earlier descriptions of widespread brain recombination when crossing *Nestin:Cre* with reporter mice.[22] Brain regions showing complete loss of ERK2 immunoreactivity included neocortex, the majority of hippocampal regions, thalamus, basal ganglia, and midbrain structures. Endothlial cells and cells consistent with microglia retained ERK2 immunoreactivity, as expected of nonneural cells (Figure 1G). ERK2 immunoreactivity was consistently not completely eliminated from some brain regions, including a subset of hippocampal CA3 neurons and in the hypothalamus (Figure 1E). There are two possible explanations for incomplete Cre-mediated recombination. Nestin promoter activity may not be sufficiently strong in some neural precursor populations to drive Cre-mediated expression, and this incomplete recombination could have been overlooked by previous reports, which used only positive reporters of recombination (GFP or β-galactosidase). Another possibility is that the floxed ERK2 allele is inaccessible (due, for example, to chromatin modification) in specific subpopulations of cells despite Nestin-driven Cre expression. Our finding of reproducible and discrete subregions that fail to undergo *Nestin:Cre*-driven recombination indicates the need for careful documentation at the cellular level of loss of protein in the cell type and/or brain region under study. Importantly, however, the phenotype that we describe occurs almost exclusively in the frontoparietal cortex, an area with complete loss of neural ERK2.

Normal Brain Development and Architecture in ERK2 cKO Mice

ERK2 cKO mice (both homozygotes and heterozygotes) show normal (equal to wild-type littermates) brain size/weight (Figure 1H) and cortical thickness (Figure 1I) at all times examined: postnatal day 2, 21, 5 weeks, 6 months, and 1 year (Figure 1). Adult brain architecture was systematically assessed on serial coronal MRI scans of three cKO and three wild-type mice. Careful side-by-side inspection of a complete series of coronal sections revealed no detectable anatomical abnormalities (Supplemental Figure S1, see *http://ajp.amjpathol.org*). Additionally, imaging postgadolinium injections revealed no evidence of abnormal vascular permeability. ERK2 cKO mice showed

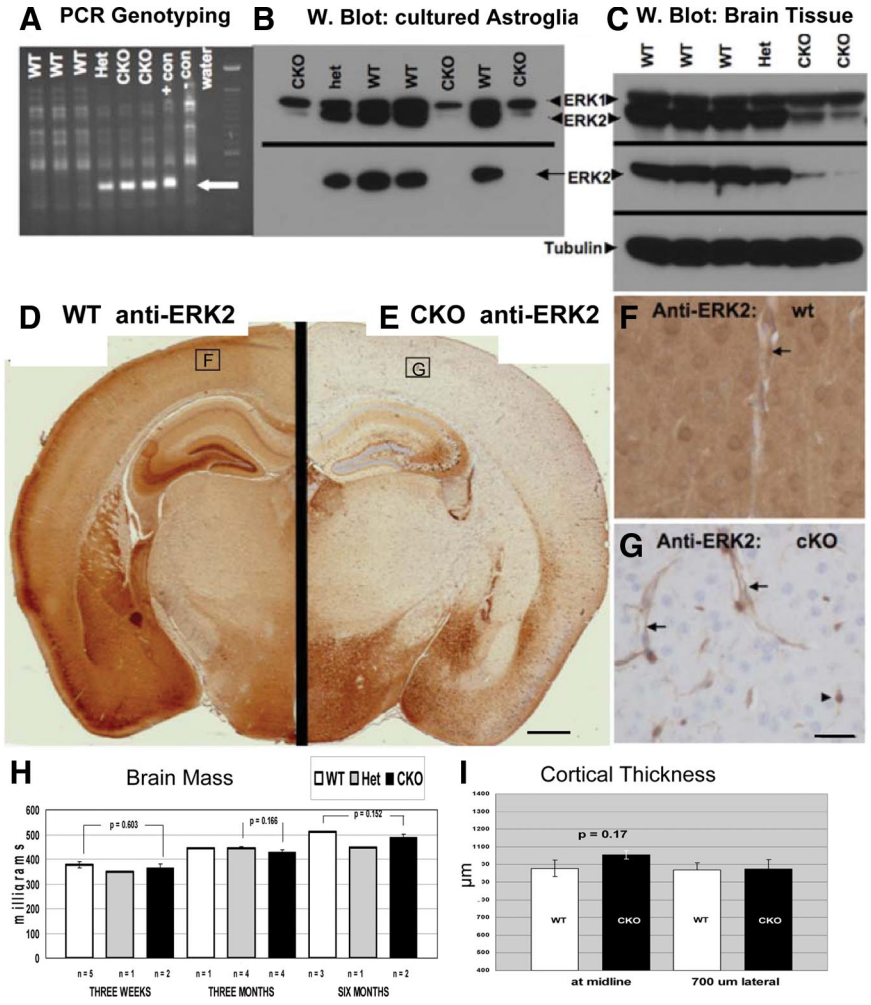

Figure 1. Conditional deletion of ERK2 from the CNS via Nestin:Cre-mediated recombination. **A:** PCR assay for recombination at the floxed ERK2 locus. DNA extracted from the cerebellum of 3-week-old littermates was amplified using primers flanking ERK2 exon 2. A 350-bp product, indicating loxP-directed deletion of the allele, is detected in both heterozgous (Het) and homozygous knockouts (CKO), as well as in a positive control sample (ERK2fl/fl astrocytes infected with Adeno-Cre (+con)). **B:** Western blot reveals ERK2 protein loss from cultured neonatal astrocytes. Total ERK1/2 (**upper panel**) blotting reveals selective loss of ERK2, but not ERK1, in cKO cells. An ERK2-specific antibody (**lower panel**) demonstrates complete loss of ERK2 in cKO cells. **C:** Western blotting of brain tissue from 3-week-old littermates reveals selective reduction of ERK2 in cKO mice, with no apparent compensatory ERK1 up-regulation. **D–G:** Immunohistochemical demonstration of loss of ERK2 immunoreactivity in ERK2 cKO cortex. Coronal sections of 3-week-old littermates (taken 1.80 mm caudal to Bregma) were stained in parallel using an ERK2-specific antibody. Whereas wild-type (WT) cortex exhibits intense ERK2 immunostaining in cortical neurons and neuropil (**D**), cKO mice show complete loss of cortical neuropil immunoreactivity (**E**). Some brain regions, including hippocampal CA2/3 and hypothalamus, consistently show retention of some ERK2 immunoreactivity (**E**). Higher power images of cortical ERK2 staining (corresponding to the boxed regions in **D** and **E**) reveal neuronal, neuropil, and vascular staining in the WT (**F**). As expected from a Nestin:Cre-driven recombination, neuronal and neuropil ERK2 is eliminated in the cKO cortex, whereas endothelial (**arrows**) and probable microglial (**arrowhead**) expression is retained (**G**). Neither brain mass (**H**) nor frontal cerebral cortex thickness (**I**) is affected in ERK2 cKO mice. Scale bar in G represents 25 μm, applies to **F** and **G**.

qualitatively normal motor behavior, activity, and cage behavior and reproduced normally. Quantitative behavioral assays (open-field activity monitoring, tail-hang test and circadian activity measurement) showed no significant differences between cKO mice and wild-type littermates (Supplemental Figure S2, see *http://ajp.amjpathol.org*).

Synaptogenesis, examined by immunostaining and immunoblotting for the synaptic vesicle protein SV2, revealed no qualitative decrease in staining intensity or in presynaptic puncta density nor any quantitative decrease in SV2 abundance. (Supplemental Figure S3, see *http://ajp.amjpathol.org*). MAP2 immunostaining revealed no differences in somatodendritic cytoarchitecture between cKO and control brains in cortex, basal ganglia, thalamus, hippocampus, or cerebellum (Supplemental Figure S3, see *http://ajp.amjpathol.org*).

Early-Onset and Progressive Cortical Astrogliosis in ERK2 cKO Mice

Immunohistochemistry revealed a consistent elevation of GFAP in cKO mice, restricted to the cerebral cortex (Figure 2, A–D) Wild-type mice typically show very few GFAP-positive astrocytes in cortical gray matter in the absence of injury or neurodegeneration. cKO cortices, on the other hand, contained numerous GFAP-positive astroglia, many of which showed a prominent pericapillary localization with extensive wrapping of end feet around capillaries. Western blot analysis of dissected frontal cortices confirmed elevation of GFAP at the protein level. Because elevated cortical GFAP in adult mice is usually a sign of neuronal injury or distress, we carefully studied cKO brains with a variety of markers for neuronal injury or degeneration Immunohistochemical stains for neurodegeneration-associated proteins (including tau (total and phospho-), synuclein, β-amyloid, phospho- and dephospho-neurofilament and ubiquitin) as well as Fluorojade-B failed to reveal any signs of neurodegeneration in any cKO brain regions at 5 weeks or 6 months of age.

No evidence of microglial activation in the affected cortical region was observed by immunostaining for CD11b, known to be up-regulated in reactive microglia (Figure 2, E and F). Microglia showed no morphological evidence of activation (thickened/retracted processes or amoeboid transformation). Densitometric assessment of GFAP immunohistochemistry revealed elevation in cKO mice as early as postnatal day 35, increasing with age to 6 months (Figure 3, A and B). Although GFAP immunoreactivity increases in the course of normal aging (com-

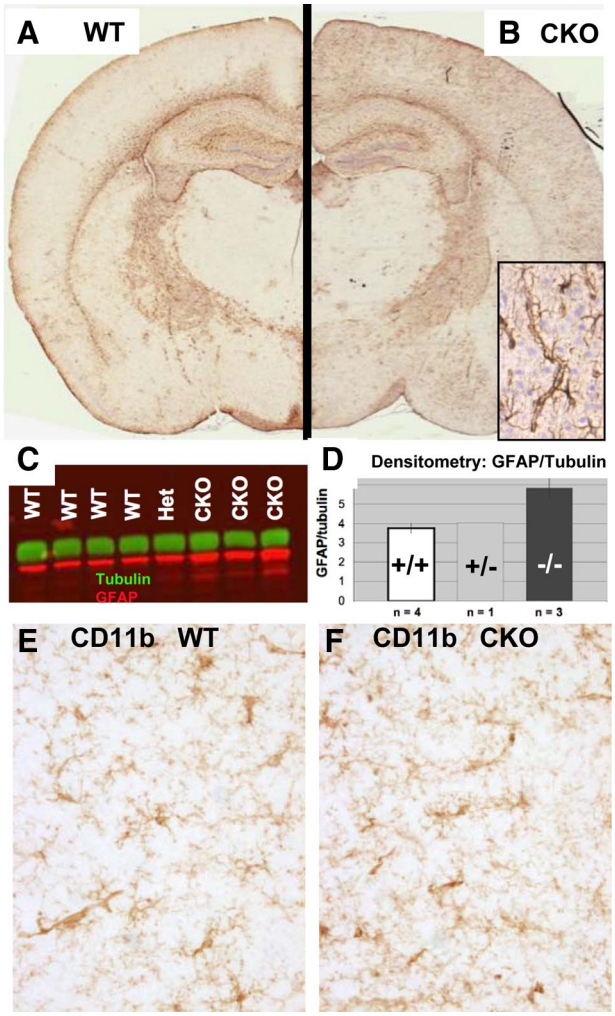

Figure 2. Cortical GFAP is selectively up-regulated in ERK2 cKO mice. **A** and **B:** Coronal sections of 6-week-old wild-type (WT) and cKO mice were processed identically for GFAP immunohistochemistry. A selective increase in GFAP immunoreactivity is apparent in the cortex of a cKO mouse (**B**) compared with a WT littermate (**A**), predominantly in perivascular astrocytes (**corner inset**, **B**). **C:** Increased cortical GFAP protein was detected by Western blot in ERK2 cKO mice. Densitometry (**D**) shows a statistically significant ($P < 0.05$) increase in GFAP (red) band intensity, normalized to α-tubulin (green) in frontal cortex of cKO mice compared with WT littermates. CD11b immunohistochemistry reveals no evidence of microglial activation in cortical regions showing elevated GFAP (**E** and **F**).

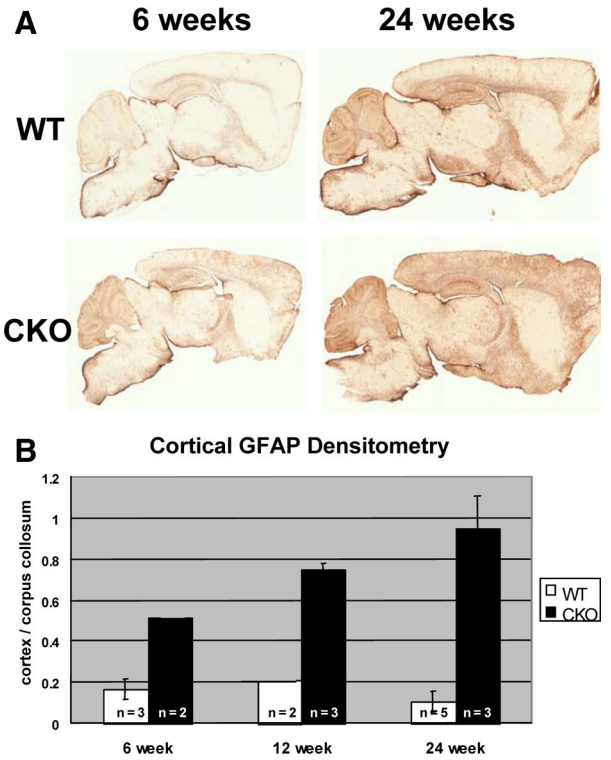

Figure 3. Progressive cortical astrogliosis in aging ERK2 cKO mice. Control mice (**upper pair**, **A**) show a mild age-dependent increase in cortical GFAP immunoreactivity. However, when normalized to white matter (corpus callosum) GFAP immunoreactivity, there is no evidence of a cortex-specific increase (**B**, white bars). ERK2 cKO mice show markedly increased cortical GFAP between 6 and 24 weeks (**A**, **lower pair**). Quantification of the cortex/corpus callosum ratio indicates a cortex-specific increase in GFAP with aging (**B**, black bars). Error bars represent SEM.

pare Figure 3A wild-type 42 days to 180 days), we found that the ratio of cortical to white matter (corpus callosum) GFAP remains stable in control mice. In contrast, there is a cortex-specific increase in GFAP in aging cKO mice, as revealed by a progressive increase in the cortical/corpus callosum GFAP intensity. The cortex/corpus callosum GFAP immunoreactivity ratio is significantly greater in ERK2 cKO frontal cortex than wild-type littermates at 24 weeks of age ($P < 0.05$, Students' *t*-test; Figure 3B). Other markers of astrogliosis, such as vimentin or nestin, up-regulation were absent (data not shown). In addition, no evidence for increased astroglial proliferation was found in the affected cortical regions (5-bromo-2′-deoxyuridine incorporation experiments; data not shown).

Parenchymal and Perivascular Collagen-Containing Fibrils Accumulate in ERK2 cKO Cortex

Although numerous markers for neuronal degeneration were negative, application of the Gallyas silver degeneration stain (Nadler's modification)[18] unexpectedly revealed the presence of numerous parenchymal fibrils, concentrated in the frontoparietal cortex of all (11 of 11) cKO brains (Figure 4, A–D). The Gallyas silver degeneration stain is generally used to visualize degenerating synaptic terminals, processes, and cell bodies of neurons that become argyrophilic during the course of cell death by unknown biochemical mechanisms. Fibrils were never seen in wild-type nor heterozygous KO littermates, which were confirmed to have partially reduced ERK2 levels, indicating a recessive inheritance pattern. Morphometry of 300 Gallyas-stained fibrils in 40-μm-thick free floating sections from three different cKO mice revealed a mean length of 9.92 $\pm$ 4.88 μm (SD) in length (range, 2.4 to 28.7 μm) and a mean diameter of 0.237 μm $\pm$ 0.058. Wilder's reticulin stain, a silver deposition method widely used to stain collagen, revealed not only the parenchymal fibrils labeled by Gallyas stain but also revealed a markedly increased pericapillary reticulin matrix surrounding virtually all cortical gray matter capillaries in cKO brains (Figure 4, E–G). Thus, these two silver stains reveal two distinct kinds of aberrant matrix in the

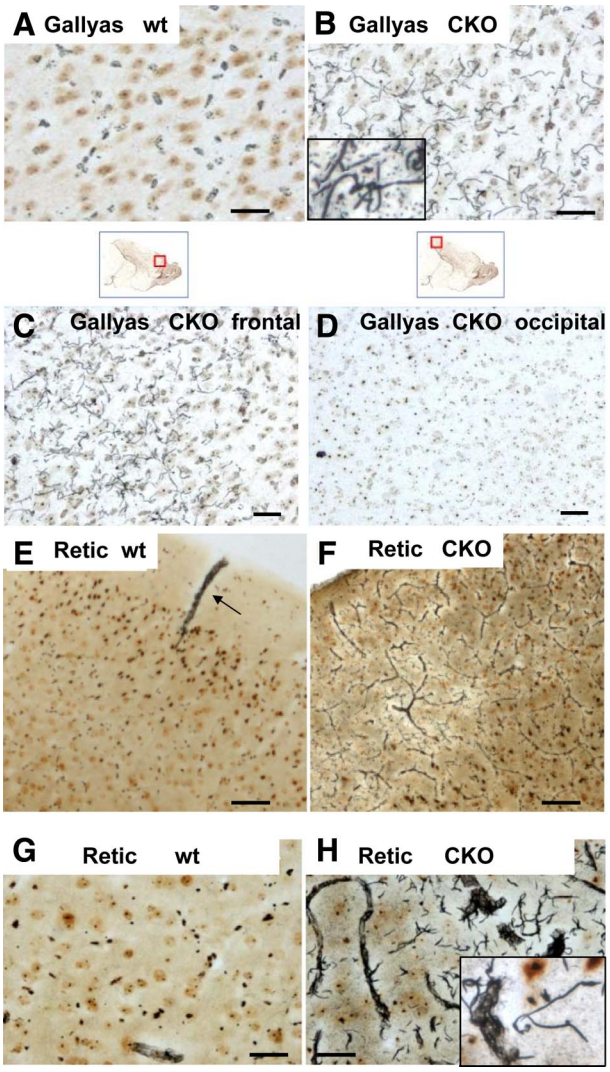

Figure 4. Parenchymal and perivascular collagen-containing fibrils accumulate selectively in ERK2 cKO frontal cortex. **A:** Gallyas silver degeneration stain reveals numerous wavy parenchymal fibrils in cKO frontal cortex (**B**) but not in controls (**A**). Aberrant fibrils are abundant in the frontoparietal cortex (**C**) of a 6-week-old ERK2 cKO mice and completely absent from occipital cortex (**D**) of the same animal. Reticulin staining (**E–H**) reveals, in addition to the isolated parenchymal fibrils highlighted by Gallyas stain, abundant pericapillary matrix material in cKO cortex (**F** and **H**). Wild-type (wt) animals show reticulin-positive matrix material restricted to large penetrating arteries/arterioles in superficial cortex (**arrow**, **E**). Scale bars represent 50 μm (**A**, **B**, **G**, and **H**), 100 μm (**C–F**), and 1 μm (**G**).

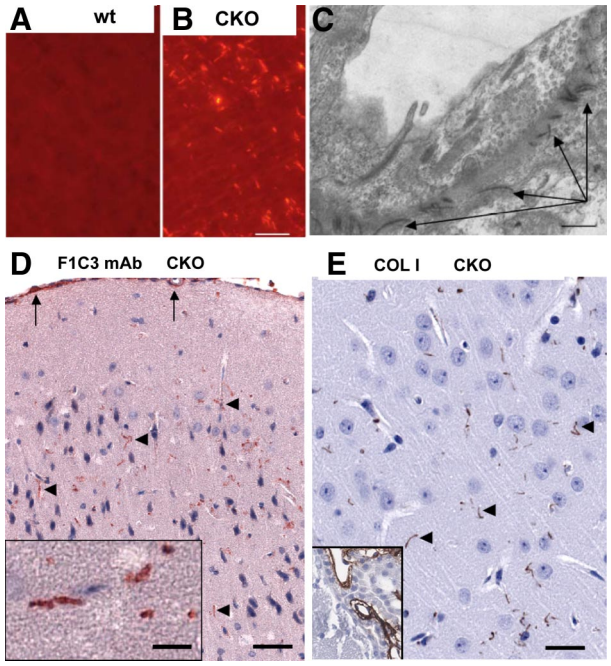

Figure 5. Histochemical and Immunohistochemical demonstration of collagen fibrils in cKO cortex. Sirius Red staining with polarized illumination reveals collagen fibrils in cKO cortex (**B**) but not littermate controls (**A**). Electron microscopy (**C**) reveals pericapillary collagen fibrils (**arrows**) in cKO cortex, not seen in control pericapillary matrix. **D:** Monoclonal antibody F1C3, specific for a conserved epitope on collagens I, III, and V, shows selective staining of parenchymal fibrils (**arrowheads**) in ERK2 cKO mice. Pial surface and vascular F1C3 immunoreactivity (**arrows**) was present in cKO as well as wild type cortex. **E:** Affinity-purified anti-collagen I antibody also labels parenchymal fibrils (**arrowheads**) in cKO cortex. Choroid plexus, known to contain abundant fibrillar collagen, serves as an internal positive control (**corner inset, E**) detected in both cKO and wt mice. Scale bars represent 50 μm (**A, B, D, E**) and 1 μm (**C**).

cKO brains: parenchymal fibrils, which are both Reticulin positive and Gallyas positive, and perivascular matrix material, which is Reticulin positive but Gallyas negative.

Reticulin and Gallyas silver deposition stains, although highly sensitive, are not specific for collagen or any single matrix protein. To provide more specific evidence of collagen deposition, brain sections were stained with Sirius Red, considered a specific collagen stain.[24,25] Parenchymal fibrils showed bright red fluorescence when viewed with polarizing filters (Figure 5, A and B), a property suggested to be specific for type I collagen, compared with the green birefringence characteristic of type III (cartilagenous) collagens.[24]

Electron microscopy was performed on portions of frontal cortex of 6-week-old ERK2 cKO mice as well as control littermates. There was no evidence of any neurodegeneration (nuclear condensation, membrane blebs, filamentous accumulations, increased lysosomes, abnormal organelle accumulations, or axonal swellings). The only noticeable difference between cKO and wild-type cortices was the presence of increased numbers of electron-dense collagen-like fibrils near and within the basal lamina of some cortical capillaries (Figure 5C). Similar fibrils were found in the pia/arachnoid and Virchow-Robbins spaces around large penetrating vessels in both cKO and wild-type mice, as expected.

More definitive evidence came from immunohistochemistry with two different antibodies recognizing fibrillar collagen forms (Figure 5, D and E). Both monoclonal antibody F1C3, recently proven to recognize fibrillar collagens I, III, and V,[26] and a polyclonal antibody specific for collagen I highlighted parenchymal fibrils scattered in the parenchyma but did not label pericapillary matrix. Thus, the Gallyas-positive parenchymal fibers do contain at least fibrillar collagen I, but the Reticulin-rich pericapillary matrix does not contain type I collagen but could contain other collagens.

Because the fibrils have morphological characteristics similar to Alzheimer's disease neuropil threads,[27] we performed extensive tau immunolocalization studies, including antibodies against hyperphosphorylated tau. ERK2 cKO cortical fibrils did not contain any tau-immunoreactive material, and Western blotting for tau protein (total, dephospho-, and phosphorylated forms) showed no difference between cKO and control cortex (data not shown).

Aberrant String Vessels and Up-Regulated MLC1 Indicate a More General Perturbation of the Cortical Gliovascular Unit in ERK2 cKO Mice

Immunostaining for collagen IV, a nonfibrillar collagen found in all pericapillary basement membranes, revealed abnormal string vessels in ERK2 cKO frontal cortex (Figure 6B, arrows) but not controls (Figure 6A). String vessels are poorly characterized microvascular structures, reported to be present in high numbers during brain development, suggesting that they could represent endothelial/pericyte sprouts related to angiogenesis.[28] String vessels are also reported to be increased in Alzheimer's disease.[29]

MLC1 is a membrane protein concentrated in distal perivascular astrocyte foot processes, and normally expressed at low levels in gray matter but can be up-regulated in disease states.[30–32] MLC1 immunoreactivity was upregulated in pericapillary processes in ERK2 cKO relative to wild-type cortex (Figure 6, C and D). To test the possibility that the microvascular endothelium of cKO mice showed a biochemical signature of activation, we probed sections with an antibody recognizing a phosphorylated epitope on ezrin/radixin/moesin (ERM) (phospho-ezrin (Thr567))/radixin (Thr564)/moesin (Thr558), which is phosphorylated in response to growth factor and cytokine stimulation, leading to cytoskeletal reorganization and is associated with increased microvascular permeability.[33] cKO capillaries (Figure 6F), but not wild type (Figure 6E), showed clear endothelial phospho-ERM immunoreactivity. Thus, the ERK2 cKO phenotype is not limited to aberrant fibrillar collagen deposition but encompasses a constellation of gliovascular abnormalities.

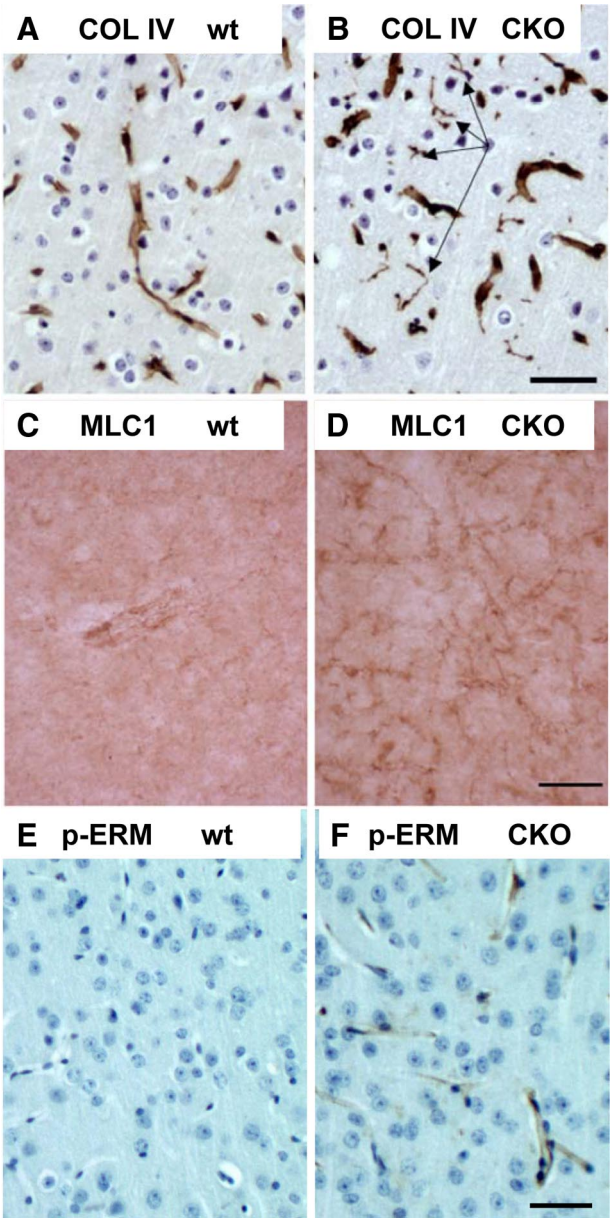

Figure 6. Evidence for microvascular abnormalities in ERK2 cKO cortex: string vessels, elevated endothelial ERM protein phosphorylation, and elevated MLC1 immunoreactivity. Collagen IV, a nonfibrillar collagen and marker of pericapillary basement membranes, reveals abnormal string vessels in ERK2 cKO cortex (**B**, **arrows**) but not controls (**A**). MLC1, a membrane protein concentrated in distal perivascular astrocyte foot processes, is up-regulated in pericapillary processes in ERK2 cKO (**D**) compared with wild-type (wt) cortex (**C**). Phospho-ERM staining, indicating possible growth factor/cytokine activation of endothelium, is up-regulated in cKO cerebral cortical capillary endothelium (**F**) compared with wild-type (wt) (**E**). Scale bars represent 50 μm.

Increased Production of Fibrillar Collagens in Cultured ERK2 cKO Astroglia

To determine whether the production of fibrillar collagens could be a cell-autonomous function of ERK2-deficient astrocytes, we prepared primary cultures from the forebrains of wild-type and ERK2 cKO mice. Immunofluorescence staining was performed with a monoclonal antibody (F1C3) previously determined to recognize a shared epitope (GPPGPVG) in fibrillar collagens I, II, and V.[34] Compared with wild-type cultures, we observed a striking increase in the fraction of cells positive for F1C3 (Figure 7). Thus, fibrillar collagen production could be under the cell-autonomous negative control of an ERK2-mediated signal.

Expression Profiling of ERK2 cKO Cerebral Cortex

To explore potential gene expression changes underlying the complex brain phenotype, we performed a genome-

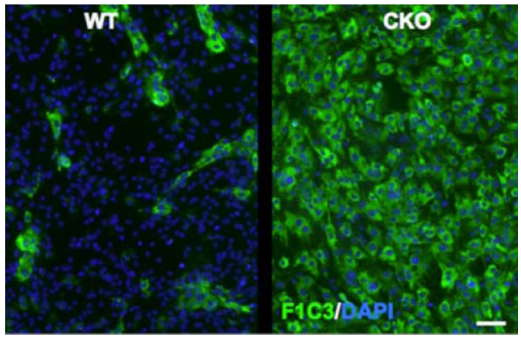

Figure 7. Elevated fibrillar collagen in ERK2 cKO primary astroglial cultures. Primary astroglial cultures derived from cKO or control littermate forebrains were labeled with mAb F1C3, recognizing an epitope shared on fibrillar collagens I/III. Scattered immunopositive cells were found in wild-type (WT) cultures (**left panel**). In contrast, virtually all cells from ERK2 cKO mice were F1C3 positive. Scale bar = 50 μm.

Table 2. Expression Profiling of ERK2 cKO Frontal Cerebral Cortex: Top 10 Up-Regulated Genes

ID	Gene_assignment	Gene symbol	RefSeq	*P* value (ERK2-CKO vs WT)	Fold change (ERK2-cKO vs WT)
10395534	XM_001472023 // 100039062 // predicted gene, 100039062 // 12 B3 12 // 100039062	100039062	XM_001472023	0.00125458	2.88604
10569344	NM_001122737 // Igf2 // insulin-like growth factor 2 // 7 F5 7 69.09 cM // 16002	*Igf2*	NM_001122737	0.0423139	2.65605
10541318	NM_144512 // Slc6a13 // solute carrier family 6 (neurotransmitter transporter, G	*Slc6a13*	NM_144512	0.00355848	2.05448
10506110	NM_001081202 // L1td1 // LINE-1 type transposase domain containing 1 // 4 C6 //	*L1td1*	NM_001081202	0.0258555	1.99487
10483326	NM_018852 // Scn9a // sodium channel, voltage-gated, type IX, α // 2 C1.3 2	*Scn9a*	NM_018852	0.04023	1.94137
10552299	NM_183166 // EG233164 // predicted gene, EG233164 // 7 B3 7 // 233164 /// ENSMUS	*EG233164*	NM_183166	0.0393063	1.85383
10487605	NM_177653 // F830045P16Rik // RIKEN cDNA F830045P16 gene // 2 F1 // 228592 /// E	*F830045P16Rik*	NM_177653	0.0418857	1.82114
10501433	NM_177091 // Fndc7 // fibronectin type III domain containing 7 // 3 F3 // 320181	*Fndc7*	NM_177091	0.0315276	1.80687
10444674	NM_023463 // Ly6g6c // lymphocyte antigen 6 complex, locus G6C // 17 B1 // 68468	*Ly6g6c*	NM_023463	0.03225	1.80364
10559667	NM_008350 // Il11 // interleukin 11 // 7 A1 7 2.0 cM // 16156 /// U03421 // Il11	*Il11*	NM_008350	0.0367704	1.80146

Differential mRNA expression between ERK2 cKO ($n = 3$) and littermate control (WT, $n = 3$) frontal cerebral cortex was assessed by microarray analysis using Affymetrix whole genome GeneChip Mouse Gene 1.0 ST arrays. WT, wild type.

wide microarray analysis, comparing frontal cortex from three homozygous null (ERK2 cKO) mice with three normal littermates (wild type). Independent hybridizations of the three ERK2cKO and three wild-type samples on Affymetrix whole-genome GeneChip Mouse Gene 1.0 ST arrays revealed 391 differentially regulated genes (analysis of variance, $P < 0.01$). All raw and processed datasets are publicly available at *https://discovery.genome.duke.edu* (project number 1906; free registration is required to access data). The top 10 up- and down-regulated genes are listed in Tables 2 and 3, respectively. GeneGo MetaCore (GeneGo, Encenitas, CA) functional analysis of all 391 significantly ($P < 0.01$) altered genes revealed the most significantly altered cellular process network in ERK2 cKO brain as "Proteolysis/Extracellular Matrix Remodeling" ($P = 5.048e\text{-}04$) and the most significantly altered pathway map as "Development/Neurotrophin Signaling" ($P = 2.421e\text{-}05$). Three of the genes most up-regulated in ERK2 cKO cortex are known to be enriched in astrocytes: Slc6a13 (2.05-fold up-regulated) also known as the γ-aminobutyric acid transporter GAT3;[35] interleukin-11 (1.80-fold up-regulated in ERK2 cKO cortex);[36] and Aldh1A1 (1.5-fold increased in ERK2 cKO cortex).[37] One collagen gene, Col2a1, was significantly ($P < 0.01$) but modestly up-regulated (1.30-fold increased in ERK2cKO cortex). Although collagen II is best studied in cartilage biology, Col2a1 expression is documented in the brain parenchyma.[38] Future studies will address the possible accumulation of collagen II isoforms in the brain of ERK2cKO mice and more generally in mouse models and human disease states exhibiting pathology of the gliovascular unit.

Specificity of the Phenotype for ERK2 Loss: No Fibrils in ERK1 KO Mice

We asked whether deletion of the closely related MAPK, ERK1, would also result in cortical collagen fibril formation and astrogliosis. ERK1 KO mice, which are viable and fertile, have grossly and histologically normal brain architecture but exhibit subtle electrophysiological deficits.[39] We found no evidence of any fibril formation nor elevated cortical GFAP immunoreactivity in ERK1 KO mice, indicating the exquisite specificity of the phenotype for ERK2 loss of function. We also considered the possibility that the phenotype could be the result of diminished neurotrophin signal-

Table 3. Expression Profiling of ERK2 cKO Frontal Cerebral Cortex: Top 10 Down-Regulated Genes

Transcript ID	Gene_assignment	Gene symbol	RefSeq	*P* value (ERK2-cKO vs WT)	Fold change (ERK2-cKO vs WT)
10503196	NM_001081417 // Chd7 // chromodomain helicase DNA binding protein 7 // 4 A1 4 1	*Chd7*	NM_001081417	0.0108441	1.98634
10514466	NM_010591 // Jun // Jun oncogene // 4 C5-C7 4 44.6 cM // 16476 /// J04115 // Jun	*Jun*	NM_010591	0.0234714	−1.84637
10427035	NM_010444 // Nr4a1 // nuclear receptor subfamily 4, group A, member 1 // 15 F //	*Nr4a1*	NM_010444	0.0234266	−1.83148
10501277	NM_175470 // Gpr61 // G protein-coupled receptor 61 // 3 F2.3 // 229714 /// BC11	*Gpr61*	NM_175470	0.0062583	−1.82963
10395409	NM_008584 // Meox2 // mesenchyme homeobox 2 // 12 A3 12 20.0 cM // 17286 /// BC0	*Meox2*	NM_008584	0.0381391	−1.79783
10555722	NM_147104 // Olfr550 // olfactory receptor 550 // — // 259108 /// BC116960 //	*Olfr550*	NM_147104	0.0213001	−1.77826
10496359	NM_016885 // Emcn // endomucin // 3 G3 // 59308 /// BC003706 // Emcn // endomuci	*Emcn*	NM_016885	0.0368348	−1.73042
10418434	NM_008407 // Itih3 // inter-α trypsin inhibitor, heavy chain 3 // 14 A2-C1 /	*Itih3*	NM_008407	0.0193124	−1.73002
10391084	NM_010404 // Hap1 // huntingtin-associated protein 1 // 11 D 11 60.0 cM // 15114	*Hap1*	NM_010404	0.0221293	−1.7291
10422244	NM_175499 // Slitrk6 // SLIT and NTRK-like family, member 6 // 14 E3 // 239250 /	*Slitrk6*	NM_175499	0.0250078	−1.69499

Differential mRNA expression between ERK2 cKO (n = 3) and littermate control (wt, n = 3) frontal cerebral cortex was assessed by microarray analysis using Affymetrix whole genome GeneChip Mouse Gene 1.0 ST arrays. WT, wild type.

ing, known to require ERK activation, by analyzing frontal cortices of brain-specific conditional TrkB KO (GFAP:Cre; TrkBfl/fl) mice.[40] No evidence of any parenchymal fibrils was observed in these mice, indicating that the ERK2 phenotype is not due to impairment of TrkB-mediated neurotrophin signaling.

Additional Genetic Evidence for Neuroglial Origin of the Gallyas-Positive Fibrils: Partial Phenocopy by GFAP:Cre but not CamKII-Cre Crosses

Despite extensive characterization in our lab and others, it is possible that Nestin:Cre could drive recombination in a small, undetected subset of mesenchymal cells, somehow causing aberrant collagen deposition. To provide independent evidence that the phenotype is due to ERK2 loss from neural cells, we examined ERK2 cKOs generated by crossing the floxed ERK2 mice with a GFAP:Cre strain.[23] Homozygous cKOs, but not control littermates from this cross, were also found to have Gallyas- and Reticulin-positive fibrils limited to frontal cortex (data not shown). The density of fibrils was lower in these mice, probably due to differences in the spatiotemporal pattern of Cre expression between Nestin:Cre and GFAP:Cre mice.[41]

To test the possibility that aberrant fibril deposition results from neuronal ERK2 deletion, we crossed the ERK2fl/fl mice with a forebrain neuron-specific Cre mouse, CamKII-Cre mice.[30] We confirmed loss of ERK2 immunoreactivity in pyramidal neurons of the cortex, basal ganglia, and hippocampus of cKO offspring. We examined cKO mice from two litters from these crosses and found no Gallyas-positive fibrils nor any increase in cortical GFAP immunoreactivity. This finding suggests that collagen fibril deposition is not a direct result of ERK2 loss from cortical pyramidal neurons, although we cannot rule out the possibility of an origin from CamKII-negative neurons or an indirect mechanism in which ERK2 loss from neural cells triggers collagen deposition by the microvasculature. Table 4 summarizes the

Table 4. Summary of Genotype/Phenotype Analyses

Mouse genotype	Cortical fibrils
C57BL/6 and Balb/C, wt background strains	
ERK1$^{-/-}$ (general KO)	
NesCre;ERK2$^{wt/wt}$	
NesCre;ERK2$^{wt/fl}$	
NesCre;ERK2$^{fl/fl}$	+++
GFAPCre;ERK2$^{wt/wt}$	
GFAPCre;ERK2$^{wt/fl}$	
GFAPCre;ERK2$^{fl/fl}$	+
CamKIICre;ERK2$^{fl/fl}$	
GFAPCre;TrkB$^{fl/fl}$	

Cortical reticulin-positive fibrils were detected in brain-specific cKOs of ERK2 driven by *Nestin:Cre* and, to a lesser degree, by *GFAP:Cre*. No such fibrils were ever observed in wild-type background strains, in heterozygous cKOs driven by *Nestin:Cre* or *GFAP:Cre*, or in conditional ERK2 KOs driven by *CamKIICre*. No fibrils were observed in a brain-specific (*GFAP:Cre*) cKO of TrkB.

various mouse lines and crosses examined in this study. A schematic diagram summarizes the complex ERK2 cKO phenotype (Figure 8).

Discussion

Nonredundant Functions for ERK2 and ERK1 in the Brain

ERK1 and ERK2 genes are highly similar (>90% amino acid identity), but their presence as distinct genes in all vertebrates strongly suggests distinct functions. Clearly, the fact that ERK1 KO mice are nearly normal but ERK2 KOs are embryonic lethal indicates a nonredundant function for ERK2. Our finding that loss of cortical ERK2 but not ERK1 causes aberrant collagen deposition and microvascular abnormalities indicates a highly selective function for ERK2. Our finding adds to the list of differential functions of these highly conserved kinases. Hepatocyte proliferation, both *in vitro* and *in vivo*, is dependent on ERK2 but not ERK1.[42] On the other hand, ERK1, but not ERK2, is responsible for *in vitro* and *in vivo* adipogenesis.[43] A series of targeted alleles in mice allowed partial knockdown of ERK2, avoiding embryonic lethality.[44] ERK2 partial knockdown mice showed impaired learning in several maze tasks, and no evidence for ERK1 up-regulation, suggesting a specific role for ERK2 in learning and memory. Two recent studies described neurodevelopmental phenotypes in CNS-specific ERK2 cKO mice. Using the GFAP:Cre strain to drive recombination in early cortical development, Samuels et al[16] found impaired neurogenesis, increased astrogliogenesis, and a modest reduction in cortical thickness in ERK2 cKO embryos. A similar study,[15] but using the Nestin:Cre strain, also found reduced neurogenesis and increased astrogliogenesis in neurosphere cultures derived from the embryonic and early postnatal ventricular zone. Neither study investigated adult cortical histopathological phenotypes. This is of clinical importance because of new work identifying distal chromosome 22q11.2 microdeletions, including the ERK2 gene, in patients with a developmental and neurocognitive syndrome.[45] Nothing is yet known about the neuropathological changes in these patients, and it will be particularly interesting to examine the cerebral cortical microvasculature.

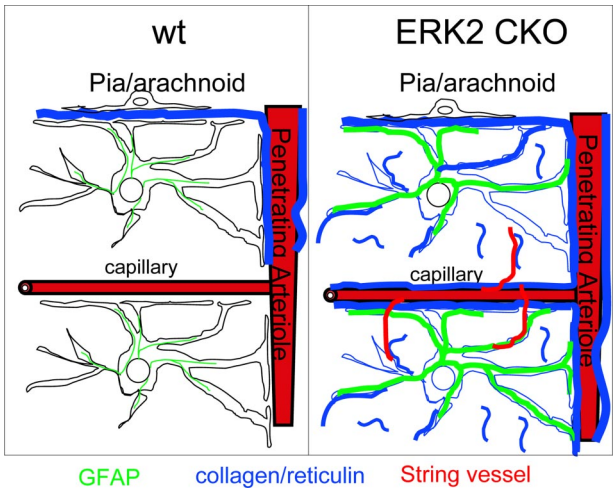

Figure 8. Schematic summary of ERK2 cKO astrovascular phenotype. In control mouse cortex (**left panel**), reticulin-positive fibrillar collagen (blue) is limited to the pia/arachnoid and Virchow-Robbins spaces surrounding penetrating arterioles. In ERK2 cKO mice (**right panel**), fibrillar collagen accumulates in parenchymal neuropil in the form of short fibrils. Additional reticulin-positive material, probably a precursor to fibrillar collagen and not recognized by mAb F1C3 or anti-collagen I antibodies, also accumulates around all cortical capillaries in cKO cortex. Abnormal string vessels are found selectively in regions with elevated fibrillar collagen deposition, and perivascular astrocytes show elevated GFAP. The results suggest a model in which pericapillary astrocytes regulate either the production or the degradation of fibril-forming collagens via an ERK2-dependent signaling pathway.

Collagen Gene Expression in the CNS: Up-Regulation in Reactive and Cultured Astrocytes and Cell-Type-Specific Profiles

More than 20 types of collagen participate in the formation of the extracellular matrix in various tissues. In the normal brain, fibrillar collagens (which include type I, II, III, V, XI and XXIV and XXVII) are only found in the pia mater (formed by meningeal cells of mesenchymal origin) and in the Virchow-Robbins perivascular spaces of larger penetrating arteries and arterioles. Collagen IV, the major sheet-forming collagen, is found in the basement membrane of all cerebral vessels, including capillaries. The accepted dogma was that collagens are expressed only by mesenchymal cells, including endothelial and meningothelial cells, thus explaining their limited distribution in the CNS. Work by Liesi et al[46–48] clearly showed that astrocytes, both in culture and *in vivo*, can synthesize and secrete basement membrane proteins, including collagen IV (nonfibrillar), fibronectin, and laminin.[30] Recent work indicates that astrocytes in culture can synthesize and secrete fibrillar collagens.[26,34] Some nonfibrillar collagens, including type XVII, are expressed by neurons.[49] In addition, gene profiling studies of fluorescence-activated cell-sorted astrocytes, oligodendroglia, and neurons confirmed differential expression of multiple collagen genes in astrocytes, as well as oligodendroglia and neurons.[37] There

is growing awareness of roles for a diversity of collagens in central nervous system development.[50]

Potential Mechanisms Linking ERK2 to Collagen Deposition

How might loss of ERK2 function lead to pericapillary and parenchymal collagen fibril deposition? Two nonexclusive mechanisms could contribute to the phenotype: 1) an ERK2-mediated *suppression* of collagen synthesis (at the transcriptional or translational level) or 2) an ERK2-mediated *stimulation* of collagen degradation. The fact that expression of several matrix metalloproteinases is regulated by ERK MAPK signaling[51,52] makes the second an attractive hypothesis. Finally, we cannot rule out the possibility that ERK2-deficient astrocytes or other neural cell types secrete a factor that induces (or fail to secrete a factor that supresses) microvascular cell production of perivascular collagens.

Roles for Astrocytes in Regulating Cerebral Microvasculature Structure and Function

Evidence that a primary defect in astrocytes can cause abnormal cerebrovascular development and a dysfunctional blood-brain barrier comes from the study of two genetically defined diseases. Duchenne's Muscular Dystrophy is an X-linked disease caused by truncation or deletion mutation of dystrophin, a large protein associated with the submembranous actin cytoskeleton. Humans with muscular dystrophy, as well as mice with targeted mutations, show, in addition to muscle degeneration, brain abnormalities and cognitive deficits.[53] Dystrophin and its associated complex of proteins are largely concentrated within the perivascular processes of astrocytes.[54] Studies on mouse models of muscular dystrophy revealed severe abnormalities in cortical microvessels, including disruption of tight junctions and leakiness of the blood-brain barrier.[55–57] Since vascular cells do not express appreciable levels of dystrophins, the mechanism of cerebrovascular dysfunction in muscular dystrophy is thought to involve faulty astrocyte-endothelial interactions. Megalencephalic leukoencephalopathy with subcortical cysts is an autosomal recessive disorder characterized by development of subcortical cysts and progressive cognitive decline. Brains of patients with this disease exhibit highly abnormal vacuolar morphology. The gene mutated in the disease, MLC1, encodes a transmembrane protein expressed almost exclusively in the distal perivascular foot processes of astrocytes.[30,58,59] Thus, astrocyte-vascular interactions are critical in the maintenance of a normal cerebral vasculature.

GFAP-transforming growth factor-β transgenic mouse provided further direct evidence that astrocytes can induce pathological changes in vascular endothelium. Overexpression of transforming growth factor-β under the control of the GFAP promoter resulted in microvascular degenerative changes highly reminiscent of those seen in Alzheimer's disease brains.[60] These changes included perivascular astrogliosis, increased accumulation of basement membrane proteins, vascular amyloidosis and endothelial cell abnormalities.

Collagen Dysregulation in Neurological Disease

The extracellular matrix of the CNS is unique among all tissues in that it normally lacks fibril-forming components.[61] In animal CNS injury models[62] as well as in human Alzheimer's disease, collagens are up-regulated both in basement membranes and focally in brain parenchyma.[63] Active multiple sclerosis plaques contain elevated levels of extracellular matrix proteins including collagens, not only in vascular walls but also within affected brain parenchyma.[64] Intriguingly, a nonamyloid protein found in a subset of Alzheimer's plaques was found to be a modified form of a transmembrane collagen.[65–67] The presence of parenchymal fibrillar collagen has been reported in human temporal lobe epilepsy.[68] Most importantly, inhibition of collagen synthesis after brain lesion prevented glial scar formation and promoted axonal regeneration and recovery of function.[69] Finally, this study adds to a growing number of mouse mutagenesis experiments revealing the complexity and diversity of molecular mechanisms underlying reactive astrogliosis.[70]

Acknowledgments

We thank Dr. Andreas Faissner (Ruhr University Bochum, Bochum, Germany) for the generous gift of mAb F1C3, Dr. Scott Zeitlin (University of Virginia) for providing CamKII-Cre mice and for help with behavioral assays, and Dr. Louis Reichardt (UCSF) for providing brain tissue from GFAP:Cre;TrkB$^{fl/fl}$ mice. We thank Dr. Ferenc Gallyas (University of Pécs, Pécs, Hungary) for thoughtful comments on the nature of the cortical fibrils and Dr. Dennis Dickson (Mayo Clinic, Jacksonville, FL) for the suggestion that Gallyas-positive fibrils could contain collagen. We thank the National Institute of Neurological Disorders and Stroke/National Institute of Mental Health Microarray Consortium (Elizabeth Salomon) for supporting the Affymetrix microarray hybridizations and analyses, performed at the Duke University Institute for Genome Sciences by Holly K. Dressman, Heather Hemric, and ZhengZheng Wei. We thank Ahmad Fashandi and George Glass for performing immunohistochemical experiments for the project.

References

1. Karasewski L, Ferreira A: MAPK signal transduction pathway mediates agrin effects on neurite elongation in cultured hippocampal neurons. J Neurobiol 2003, 55:14–24
2. Shinoda T, Taya S, Tsuboi D, Hikita T, Matsuzawa R, Kuroda S, Iwamatsu A, Kaibuchi K: DISC1 regulates neurotrophin-induced axon elongation via interaction with Grb2. J Neurosci 2007, 27:4–14
3. Dijkhuizen PA, Ghosh A: BDNF regulates primary dendrite formation in cortical neurons via the PI3-kinase and MAP kinase signaling pathways. J Neurobiol 2005, 62:278–288
4. Heffron DS, Mandell JW: Opposing roles of ERK and p38 MAP ki-

nases in FGF2-induced astroglial process extension. Mol Cell Neurosci 2005, 28:779–790
5. Sweatt JD: Mitogen-activated protein kinases in synaptic plasticity and memory. Curr Opin Neurobiol 2004, 14:311–317
6. Giovannini MG: The role of the extracellular signal-regulated kinase pathway in memory encoding. Rev Neurosci 2006, 17:619–634
7. Samuels IS, Saitta SC, Landreth GE: MAP'ing CNS development and cognition: an ERKsome process. Neuron 2009, 61:160–167
8. Carbonell WS, Mandell JW: Transient neuronal but persistent astroglial activation of ERK/MAP kinase after focal brain injury in mice. J Neurotrauma 2003, 20:327–336
9. Mandell JW, Gocan NC, Vandenberg SR: Mechanical trauma induces rapid astroglial activation of ERK/MAP kinase: evidence for a paracrine signal. Glia 2001, 34:283–295
10. Mandell JW, VandenBerg SR: ERK/MAP kinase is chronically activated in human reactive astrocytes. Neuroreport 1999, 10:3567–3572
11. Selcher JC, Nekrasova T, Paylor R, Landreth GE, Sweatt JD: Mice lacking the ERK1 isoform of MAP kinase are unimpaired in emotional learning. Learn Mem 2001, 8:11–19
12. Hatano N, Mori Y, Oh-hora M, Kosugi A, Fujikawa T, Nakai N, Niwa H, Miyazaki J, Hamaoka T, Ogata M: Essential role for ERK2 mitogen-activated protein kinase in placental development. Genes Cells 2003, 8:847–856
13. Yao Y, Li W, Wu J, Germann UA, Su MS, Kuida K, Boucher DM: Extracellular signal-regulated kinase 2 is necessary for mesoderm differentiation. Proc Natl Acad Sci USA 2003, 100:12759–12764
14. Saba-El-Leil MK, Vella FD, Vernay B, Voisin L, Chen L, Labrecque N, Ang SL, Meloche S: An essential function of the mitogen-activated protein kinase Erk2 in mouse trophoblast development. EMBO Rep 2003, 4:964–968
15. Imamura O, Satoh Y, Endo S, Takishima K: Analysis of extracellular signal-regulated kinase 2 function in neural stem/progenitor cells via nervous system-specific gene disruption. Stem Cells 2008, 26:3247–3256
16. Samuels IS, Karlo JC, Faruzzi AN, Pickering K, Herrup K, Sweatt JD, Saitta SC, Landreth GE: Deletion of ERK2 mitogen-activated protein kinase identifies its key roles in cortical neurogenesis and cognitive function. J Neurosci 2008, 28:6983–6995
17. Franciosi S, De Gasperi R, Dickstein DL, English DF, Rocher AB, Janssen WG, Christoffel D, Sosa MA, Hof PR, Buxbaum JD, Elder GA: Pepsin pretreatment allows collagen IV immunostaining of blood vessels in adult mouse brain. J Neurosci Methods 2007, 163:76–82
18. Nadler JV, Evenson DA: Use of excitatory amino acids to make axon-sparing lesions of hypothalamus. Methods Enzymol 1983, 103:393–400
19. Guntern R, Bouras C, Hof PR, Vallet PG: An improved thioflavine S method for staining neurofibrillary tangles and senile plaques in Alzheimer's disease. Experientia 1992, 48:8–10
20. Chang MS, Ariah LM, Marks A, Azmitia EC: Chronic gliosis induced by loss of S-100B: knockout mice have enhanced GFAP-immunoreactivity but blunted response to a serotonin challenge. Brain Res 2005, 1031:1–9
21. Tronche F, Kellendonk C, Kretz O, Gass P, Anlag K, Orban PC, Bock R, Klein R, Schutz G: Disruption of the glucocorticoid receptor gene in the nervous system results in reduced anxiety. Nat Genet 1999, 23:99–103
22. Dubois NC, Hofmann D, Kaloulis K, Bishop JM, Trumpp A: Nestin-Cre transgenic mouse line Nes-Cre1 mediates highly efficient Cre/loxP mediated recombination in the nervous system, kidney, and somite-derived tissues. Genesis 2006, 44:355–360
23. Zhuo L, Theis M, Alvarez-Maya I, Brenner M, Willecke K, Messing A: hGFAP-cre transgenic mice for manipulation of glial and neuronal function in vivo. Genesis 2001, 31:85–94
24. Junqueira LC, Cossermelli W, Brentani R: Differential staining of collagens type I, II and III by Sirius Red and polarization microscopy. Arch Histol Jpn 1978, 41:267–274
25. Malkusch W, Rehn B, Bruch J: Advantages of Sirius Red staining for quantitative morphometric collagen measurements in lungs. Exp Lung Res 1995, 21:67–77
26. Heck N, Garwood J, Dobbertin A, Calco V, Sirko S, Mittmann T, Eysel UT, Faissner A: Evidence for distinct leptomeningeal cell-dependent paracrine and EGF-linked autocrine regulatory pathways for suppression of fibrillar collagens in astrocytes. Mol Cell Neurosci 2007, 36:71–85
27. Markesbery WR, Wang HZ, Kowall NW, Kosik KS, McKee AC: Morphometric image analysis of neuropil threads in Alzheimer's disease. Neurobiol Aging 1993, 14:303–307
28. Challa VR, Thore CR, Moody DM, Brown WR, Anstrom JA: A three-dimensional study of brain string vessels using celloidin sections stained with anti-collagen antibodies. J Neurol Sci 2002, 203–204:165–167
29. Challa VR, Thore CR, Moody DM, Anstrom JA, Brown WR: Increase of white matter string vessels in Alzheimer's disease. J Alzheimers Dis 2004, 6:379–383; discussion 443–379
30. Teijido O, Martinez A, Pusch M, Zorzano A, Soriano E, Del Rio JA, Palacin M, Estevez R: Localization and functional analyses of the MLC1 protein involved in megalencephalic leukoencephalopathy with subcortical cysts. Hum Mol Genet 2004, 13:2581–2594
31. Boor I, Nagtegaal M, Kamphorst W, van der Valk P, Pronk JC, van Horssen J, Dinopoulos A, Bove KE, Pascual-Castroviejo I, Muntoni F, Estevez R, Scheper GC, van der Knaap MS: MLC1 is associated with the dystrophin-glycoprotein complex at astrocytic endfeet. Acta Neuropathol 2007, 114:403–410
32. Boor PK, de Groot K, Waisfisz Q, Kamphorst W, Oudejans CB, Powers JM, Pronk JC, Scheper GC, van der Knaap MS: MLC1: a novel protein in distal astroglial processes. J Neuropathol Exp Neurol 2005, 64:412–419
33. Koss M, Pfeiffer GR 2nd, Wang Y, Thomas ST, Yerukhimovich M, Gaarde WA, Doerschuk CM, Wang Q: Ezrin/radixin/moesin proteins are phosphorylated by TNF-α and modulate permeability increases in human pulmonary microvascular endothelial cells. J Immunol 2006, 176:1218–1227
34. Heck N, Garwood J, Schutte K, Fawcett J, Faissner A: Astrocytes in culture express fibrillar collagen. Glia 2003, 41:382–392
35. Minelli A, DeBiasi S, Brecha NC, Zuccarello LV, Conti F: GAT-3, a high-affinity GABA plasma membrane transporter, is localized to astrocytic processes, and it is not confined to the vicinity of GABAergic synapses in the cerebral cortex. J Neurosci 1996, 16:6255–6264
36. Zhang Y, Taveggia C, Melendez-Vasquez C, Einheber S, Raine CS, Salzer JL, Brosnan CF, John GR: Interleukin-11 potentiates oligodendrocyte survival and maturation, and myelin formation. J Neurosci 2006, 26:12174–12185
37. Cahoy JD, Emery B, Kaushal A, Foo LC, Zamanian JL, Christopherson KS, Xing Y, Lubischer JL, Krieg PA, Krupenko SA, Thompson WJ, Barres BA: A transcriptome database for astrocytes, neurons, and oligodendrocytes: a new resource for understanding brain development and function. J Neurosci 2008, 28:264–278
38. Leung KK, Ng LJ, Ho KK, Tam PP, Cheah KS: Different *cis*-regulatory DNA elements mediate developmental stage- and tissue-specific expression of the human COL2A1 gene in transgenic mice. J Cell Biol 1998, 141:1291–1300
39. Grueter BA, Gosnell HB, Olsen CM, Schramm-Sapyta NL, Nekrasova T, Landreth GE, Winder DG: Extracellular-signal regulated kinase 1-dependent metabotropic glutamate receptor 5-induced long-term depression in the bed nucleus of the stria terminalis is disrupted by cocaine administration. J Neurosci 2006, 26:3210–3219
40. Xu B, Zang K, Ruff NL, Zhang YA, McConnell SK, Stryker MP, Reichardt LF: Cortical degeneration in the absence of neurotrophin signaling: dendritic retraction and neuronal loss after removal of the receptor TrkB. Neuron 2000, 26:233–245
41. Malatesta P, Hack MA, Hartfuss E, Kettenmann H, Klinkert W, Kirchhoff F, Gotz M: Neuronal or glial progeny: regional differences in radial glia fate. Neuron 2003, 37:751–764
42. Fremin C, Ezan F, Boisselier P, Bessard A, Pages G, Pouyssegur J, Baffet G: ERK2 but not ERK1 plays a key role in hepatocyte replication: an RNAi-mediated ERK2 knockdown approach in wild-type and ERK1 null hepatocytes. Hepatology 2007, 45:1035–1045
43. Bost F, Aouadi M, Caron L, Even P, Belmonte N, Prot M, Dani C, Hofman P, Pages G, Pouyssegur J, Le Marchand-Brustel Y, Binetruy B: The extracellular signal-regulated kinase isoform ERK1 is specifically required for in vitro and in vivo adipogenesis. Diabetes 2005, 54:402–411
44. Satoh Y, Endo S, Ikeda T, Yamada K, Ito M, Kuroki M, Hiramoto T, Imamura O, Kobayashi Y, Watanabe Y, Itohara S, Takishima K: Extracellular signal-regulated kinase 2 (ERK2) knockdown mice show deficits in long-term memory; ERK2 has a specific function in learning and memory. J Neurosci 2007, 27:10765–10776
45. Newbern J, Zhong J, Wickramasinghe RS, Li X, Wu Y, Samuels I, Cherosky N, Karlo JC, O'Loughlin B, Wikenheiser J, Gargesha M,

Doughman YQ, Charron J, Ginty DD, Watanabe M, Saitta SC, Snider WD, Landreth GE: Mouse and human phenotypes indicate a critical conserved role for ERK2 signaling in neural crest development. Proc Natl Acad Sci USA 2008, 105:17115–17120
46. Liesi P, Kaakkola S, Dahl D, Vaheri A: Laminin is induced in astrocytes of adult brain by injury. EMBO J 1984, 3:683–686
47. Liesi P, Kauppila T: Induction of type IV collagen and other basement-membrane-associated proteins after spinal cord injury of the adult rat may participate in formation of the glial scar. Exp Neurol 2002, 173:31–45
48. Liesi P, Kirkwood T, Vaheri A: Fibronectin is expressed by astrocytes cultured from embryonic and early postnatal rat brain. Exp Cell Res 1986, 163:175–185
49. Seppanen A, Suuronen T, Hofmann SC, Majamaa K, Alafuzoff I: Distribution of collagen XVII in the human brain. Brain Res 2007, 1158:50–56
50. Hubert T, Grimal S, Carroll P, Fichard-Carroll A: Collagens in the developing and diseased nervous system. Cell Mol Life Sci 2008
51. Cohen M, Meisser A, Haenggeli L, Bischof P: Involvement of MAPK pathway in TNF-α-induced MMP-9 expression in human trophoblastic cells. Mol Hum Reprod 2006, 12:225–232
52. Kim SD, Yang SI, Kim HC, Shin CY, Ko KH: Inhibition of GSK-3β mediates expression of MMP-9 through ERK1/2 activation and translocation of NF-κB in rat primary astrocyte. Brain Res 2007, 1186:12–20
53. Uchino M, Teramoto H, Naoe H, Miike T, Yoshioka K, Ando M: Dystrophin and dystrophin-related protein in the central nervous system of normal controls and Duchenne muscular dystrophy. Acta Neuropathol 1994, 87:129–134
54. Uchino M, Yoshioka K, Miike T, Tokunaga M, Uyama E, Teramoto H, Naoe H, Ando M: Dystrophin and dystrophin-related protein in the brains of normal and mdx mice. Muscle Nerve 1994, 17:533–538
55. Nico B, Frigeri A, Nicchia GP, Corsi P, Ribatti D, Quondamatteo F, Herken R, Girolamo F, Marzullo A, Svelto M, Roncali L: Severe alterations of endothelial and glial cells in the blood-brain barrier of dystrophic mdx mice. Glia 2003, 42:235–251
56. Nico B, Mangieri D, Crivellato E, Longo V, De Giorgis M, Capobianco C, Corsi P, Benagiano V, Roncali L, Ribatti D: HIF activation and VEGF overexpression are coupled with ZO-1 up-phosphorylation in the brain of dystrophic mdx mouse. Brain Pathol 2007, 17:399–406
57. Nico B, Paola Nicchia G, Frigeri A, Corsi P, Mangieri D, Ribatti D, Svelto M, Roncali L: Altered blood-brain barrier development in dystrophic MDX mice. Neuroscience 2004, 125:921–935
58. Leegwater PA, Yuan BQ, van der Steen J, Mulders J, Konst AA, Boor PK, Mejaski-Bosnjak V, van der Maarel SM, Frants RR, Oudejans CB, Schutgens RB, Pronk JC, van der Knaap MS: Mutations of MLC1 (KIAA0027), encoding a putative membrane protein, cause megalencephalic leukoencephalopathy with subcortical cysts. Am J Hum Genet 2001, 68:831–838
59. Schmitt A, Gofferje V, Weber M, Meyer J, Mossner R, Lesch KP: The brain-specific protein MLC1 implicated in megalencephalic leukoencephalopathy with subcortical cysts is expressed in glial cells in the murine brain. Glia 2003, 44:283–295
60. Wyss-Coray T, Lin C, Sanan DA, Mucke L, Masliah E: Chronic overproduction of transforming growth factor-β1 by astrocytes promotes Alzheimer's disease-like microvascular degeneration in transgenic mice. Am J Pathol 2000, 156:139–150
61. Carlson SSaHS: Central nervous system. Edited by WD Comper. Amsterdam, Comper, 1996, pp. 1–23
62. Hirano S, Yonezawa T, Hasegawa H, Hattori S, Greenhill NS, Davis PF, Sage EH, Ninomiya Y: Astrocytes express type VIII collagen during the repair process of brain cold injury. Biochem Biophys Re Commun 2004, 317:437–443
63. Kalaria RN, Pax AB: Increased collagen content of cerebral microvessels in Alzheimer's disease. Brain Res 1995, 705:349–352
64. van Horssen J, Bo L, Dijkstra CD, de Vries HE: Extensive extracellular matrix depositions in active multiple sclerosis lesions. Neurobiol Dis 2006, 24:484–491
65. Hashimoto T, Wakabayashi T, Watanabe A, Kowa H, Hosoda R, Nakamura A, Kanazawa I, Arai T, Takio K, Mann DM, Iwatsubo T: CLAC: a novel Alzheimer amyloid plaque component derived from a transmembrane precursor, CLAC-P/collagen type XXV. EMBO J 2002, 21:1524–1534
66. Soderberg L, Kakuyama H, Moller A, Ito A, Winblad B, Tjernberg LO, Naslund J: Characterization of the Alzheimer's disease-associated CLAC protein and identification of an amyloid β-peptide-binding site. J Biol Chem 2005, 280:1007–1015
67. Soderberg L, Zhukareva V, Bogdanovic N, Hashimoto T, Winblad B, Iwatsubo T, Lee VM, Trojanowski JQ, Naslund J: Molecular identification of AMY, an Alzheimer disease amyloid-associated protein. J Neuropathol Exp Neurol 2003, 62:1108–1117
68. Veznedaroglu E, Van Bockstaele EJ, O'Connor MJ: Extravascular collagen in the human epileptic brain: a potential substrate for aberrant cell migration in cases of temporal lobe epilepsy. J Neurosurg 2002, 97:1125–1130
69. Kawano H, Li HP, Sango K, Kawamura K, Raisman G: Inhibition of collagen synthesis overrides the age-related failure of regeneration of nigrostriatal dopaminergic axons. J Neurosci Res 2005, 80:191–202
70. Correa-Cerro LS, Mandell JW: Molecular mechanisms of astrogliosis: new approaches with mouse genetics. J Neuropathol Exp Neurol 2007, 66:169–176